Available online at www.sciencedirect.com
ScienceDirect
Journal of Photochemistry and Photobiology A: Chemistry 182 (2006) 330–334
Journal of Photochemistry and Photobiology A:Chemistry
www.elsevier.com/locate/jphotochem

Laser ablation-based synthesis of functionalized colloidal nanomaterials in biocompatible solutions

Andrei V. Kabashin *, Michel Meunier

Department of Engineering Physics, Ecole Polytechnique de Montreal, Case Postale 6079, Succ. Centre-ville, Montreal, Que., Canada H3C 3A7

Available online 28 July 2006

Abstract

An overview of experimental results related to the femtosecond laser ablation-based nanofabrication in aqueous biocompatible solutions is presented. The method makes possible the production of stable metal nanoparticle colloids with extremely small size (down to 2–2.5 nm) and size dispersion (down to 1–1.5 nm). Being prepared in the absence of toxic by-products in biologically-friendly environment, the nanoparticles exhibit unique surface chemistry and can be linked to different species (oligosaccharides, biopolymers, etc.). The nanoparticles promise a solution of toxicity problem, typical for nanomaterials synthesized by pure chemical routes, and can be used in biosensing and imaging applications.

Keywords: Femtosecond laser ablation; Colloidal nanoparticles; Aqueous biocompatible solutions

1. Introduction

At present, there is an explosive growth of interest to the fabrication of nanomaterials in liquid environment due to newly emerged biosensing and bioimaging applications. Here, two classes of nanomaterials are of particular importance. The first one is related to fluorescent inorganic materials, which can be used as markers or labels of biological species. In this case, an attachment of the species to the surface (biosensing applications) or their presence in a living organism (bioimaging applications) can be screened by a fluorescent signal from the label. The second class is related to metallic or plasmonics nanostructures. The ability of noble metals to support surface plasmons gives rise to novel effects such as the appearance of peaks in absorption spectra, whose position depend on the size and the shape of nanoparticles, as well as on the average distance between them [1,2]. When used as labels of biomaterials, metal nanoparticles also make possible the control of biointeractions on the surface or in a solution by monitoring absorption spectra characteristics. Ideally, colloidal nanoparticles are supposed to have the following characteristics: (i) they must be formed in an aqueous solution; (ii) they must be small enough (1–50 nm), with a relatively narrow size dispersion; (iii) they must be free of toxic impurities on the surface; (iv) they must contain reactive chemical groups to simplify subsequent attachment to biomolecules.

In principle, colloidal semiconductor and metal nanoparticles can be routinely produced by chemical reduction methods (micelles, organometallic procedures) (see, e.g., [3–6]). However, conventional wet chemical procedures such as, e.g., the reduction of a precursor salt with a reducing agent, generally result in a surface contamination, mainly by residual anions and the reducing agent [7]. In addition, in the presence of UV radiation the oxidation of some chemically prepared materials often leads to a citoxicity of synthesized materials [8]. All these problems strongly complicate the use of chemically prepared particles in biosensing and especially in vivo imaging applications [9].

Laser ablation in liquids, which consists in the pulverization of a solid target in liquid ambience, gives a unique opportunity to solve the toxicity problem. In contrast to chemical nanofabrication methods, laser ablation can be performed in a clean, well-controlled environment such as deionized water, giving rise to the production of ultrapure nanomaterials. Most experiments were carried out with the use of nanosecond laser pulses [10–17] and the size distribution of the nanoparticles in liquids tended to be broadened since coalescence of ablated nanoclusters could not be easily overcome. To reduce the size of produced particles, aqueous solutions of surfactants such as sodium dodecyl sulfate (SDS) or CTAB were used, which covered the surface of nanoparticles and thus prevented them from the coalescence

* Corresponding author. Tel.: +1 514 340 4711x4634; fax: +1 514 340 3218.
E-mail address: andrei.kabashin@polymtl.ca (A.V. Kabashin).

1010-6030/$ – see front matter © 2006 Elsevier B.V. All rights reserved.
doi:10.1016/j.jphotochem.2006.06.008

[12–15]. This method enabled the reduction of both the mean size and size dispersion of Au and Ag nanoparticles down to 4–8 and 5 nm, respectively [12,14]. However, biosensing and imaging applications of gold nanoparticles covered with SDS or other surfactants are still problematical since surfactants complicate the subsequent biomolecule immobilization step. In addition, most of these materials are hardly biocompatible.

Modifying laser ablation-based nanoparticle synthesis method, we recently showed a possibility of producing biocompatible metal nanoparticles with very small size (down to 2 nm) and a narrow size dispersion (down to 1 nm full width at half maximum) [18–23]. This result was achieved by a combination of two factors: (i) the use of *ultrashort pulsed laser* radiation to ablate materials; (ii) use of aqueous solutions of novel biocompatible materials to control the growth and stabilize colloids. In this paper, we summarize data on properties of colloidal gold nanoparticles prepared by the femtosecond laser ablation.

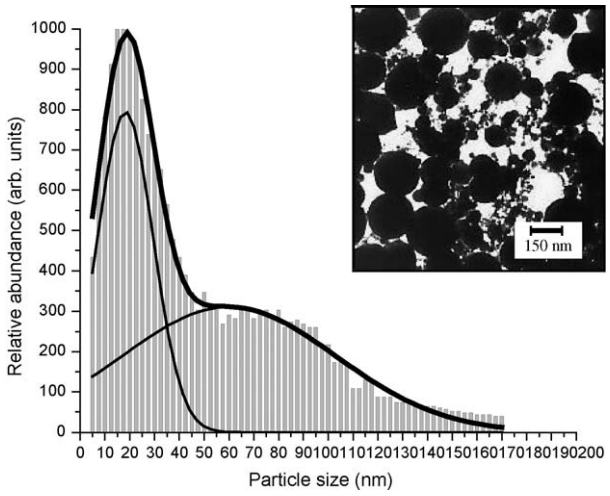

Fig. 1. TEM micrograph image and corresponding size distribution of gold nanoparticles prepared by the femtosecond laser ablation in pure deionized water at 0.2 mJ/pulse.

2. Experimental setup

The experiments were carried out with a Ti/Sapphire laser (Hurricane, Spectra Physics Lasers, Mountain View, CA), which provided 110 fs full width at half maximum (FWHM) pulses (wavelength 800 nm, maximum energy 1 mJ/pulse, repetition rate of 1 kHz). The radiation was focused by an objective with the focal distance of 7.5 cm onto a target, which was placed on the bottom of a 3-mL glass vessel filled with different aqueous solutions. The thickness of the liquid layer above the rod was about 12 mm. The vessel was placed on a horizontal platform, which executed repetitive circular motions at a constant speed of 0.5 mm/s to form circle- like ablated region on the target surface.

A gold rod with the diameter of 6 mm and the height of 6 mm was used as a target in the experiments. The ablation experiments were carried out in pure deionized water and in aqueous solutions of different materials: cyclodextrins (α-cyclodextrin, β-CD and γ-CD), biopolymers, salts, etc. All solutions were prepared from high-purity deionized water immediately prior to their use. The concentration of chemicals was varied in different experiments.

3. Results

3.1. Properties of gold nanoparticles prepared in water

To understand basic properties of nanoparticles produced by *ultrashort pulsed laser* ablation, the experiments were first carried out in neutral surfactant-free environment of pure deionized water. Here, drastically different properties of nanoparticles were obtained compared to nanosecond laser pulses. Although the mean size and size dispersion of nanoparticles were relatively large in most cases, the femtosecond laser ablation enabled to finely control these parameters by varying laser intensity of the target surface. In particular, the mean particle size could be reduced from 120 to 4 nm when the laser fluence was finely decreased down to ablation threshold values [19]. Here, two different populations of nanoparticles (low and highly size-dispersed ones) were revealed, as shown in Fig. 1, whose appearance was attributed to photon- and plasma-induced ablation mechanisms, respectively (details on the analysis of nanoparticle size distributions in deionized water and mechanisms of material ablation, can be found in [19,23]). Despite the establishment of possibilities for purely physical nanoparticle size reduction, this method does not make possible the production of small and low dispersed nanoparticles in large quantities because of too small radiation energy per pulse (the production of nanoparticles with the mean size of few usually takes hours of the experiment). Therefore, medium fluence regime (0.2 mJ/pulse) was basically used to provide a good compromise between the relatively small nanoparticle size and the relatively high production efficiency. As shown in Fig. 1, this fluence provides a broad size distribution component centered at 60 nm with the dispersion of 40–50 nm FWHM.

As we found from XPS and FTIR studies, the particles produced were partially oxidized. In particular, a high resolution XPS spectrum of the Au4f core level could be characterized by three pairs of peaks due to $Au4f_{7/2}$ and $Au4f_{5/2}$ spin-orbit coupling. While the positions of the first and most important pair (BEs of 84 and 87.3 eV) are related to elemental gold (Au^0), those of the other pairs are related to the only two stable gold oxide states, Au^+ (BEs of 85.6 and 89.1 eV) and Au^{3+} (BEs of 87.3 and 90.4 eV) [20,22]. Based on relative peak areas, their respective atomic percentages were estimated as 88.7% for Au^0, 6.6% for Au^+ and 4.7% for Au^{3+}. FTIR spectra of gold nanoparticles exhibited a broad peak in the region 3000–3600 cm^{-1}, which is attributed to OH stretching [22]. The other three peaks, centered at 1000, 1334 and 1595 cm^{-1}, are assigned to the stretching modes of carbonato (CO_3) complexes coordinated to a metal [24]. The presence of these chemical groups on the gold particle surface indicates the presence of Au–O compounds. Details on XPS and FTIR measurements can be found in [20,22].

We also found that the oxidized surface of gold nanoparticles can have different termination, depending on the pH of the environment. This conclusion followed from the zeta potential studies of gold particles produced in 10 mM NaCl (pHs were adjusted with HCl or NaOH). The particles produced were neg-

atively charged for all samples in the pH range explored. The absolute value of the zeta potential below pH 5.8 decreased as the pH decreased whereas, above pH 5.8, the absolute value of the zeta potential became almost constant. The experiments below pH 5.8 were accompanied by a much faster agglomeration of the gold colloids. This process was especially pronounced at pH 3, where agglomeration occurred during particle fabrication. Faster agglomeration is consistent with the measured decrease of the surface charge, leading to a reduction of the electrostatic repulsion between negatively charged nanoparticles. The measurement of the zeta potential of the particles as a function of pH confirms the presence of hydroxyl groups on the Au particles surface. Indeed, hydroxyl groups (–OH) are in equilibrium with $–O^-$ and their relative abundance is dictated by the pH value of their environment relative to the pK value of the hydroxylated surface. When the pH is below the pK value, –OH is dominant, and when the pH is above, $–O^-$ is dominant. Under our experimental conditions, the oxidized portion of the gold surface should almost exclusively have Au–O^- groups at pH > 5.8 and increasing numbers of Au–OH groups at pH < 5.8.

3.2. Use of biocompatible compounds to control nanoparticle growth: fabrication of functionalized nanoparticles

As showed in last paragraph, nanoparticles produced by the femtosecond laser ablation in aqueous solutions are partially oxidized and can have either OH or O^- groups on the surface. Being quite different compared to conventional colloidal nanoparticles prepared by chemical reduction methods [3], such surface chemistry opens up novel opportunities for chemical manipulations. In this paragraph, we will review properties of gold nanoparticles formed in the presence of chemical substances having different reactive groups.

3.2.1. Thiol group

To study the influence of thiol-containing group on the nanoparticle synthesis process, we performed laser ablation experiments in the presence of 3-mercaptopropionic acid (3-MPA, >99%, Sigma–Aldrich). However, our tests showed that 3-MPA hardly affected the process and was unable to stop the formation of large particles, associated with the second hardly dispersed population of nanoparticles (Fig. 1). It was a surprise since the thiol group is known as the best chemical reagent to stabilize the gold colloids. We believe that such a discrepancy of results for laser-ablated nanoparticles compared to chemically synthesized ones can be explained by a partial oxidation of their surface, which reduced the efficiency of Au–thiol interaction.

3.2.2. OH group

To understand the influence of OH group, we carried our laser ablation experiments in the presence of oligosaccharides and different biopolymers (dextran, polyethylene glycol (PEG)). In particular, very impressive results were obtained using cyclodextrins (α-cyclodextrin (CD), β-CD and γ-CD). CDs are torus-like macrocycles built up from D-(+)-glucopyranose units, which are linked by α-1-4-linkages (the most common ones are α, β and γ-

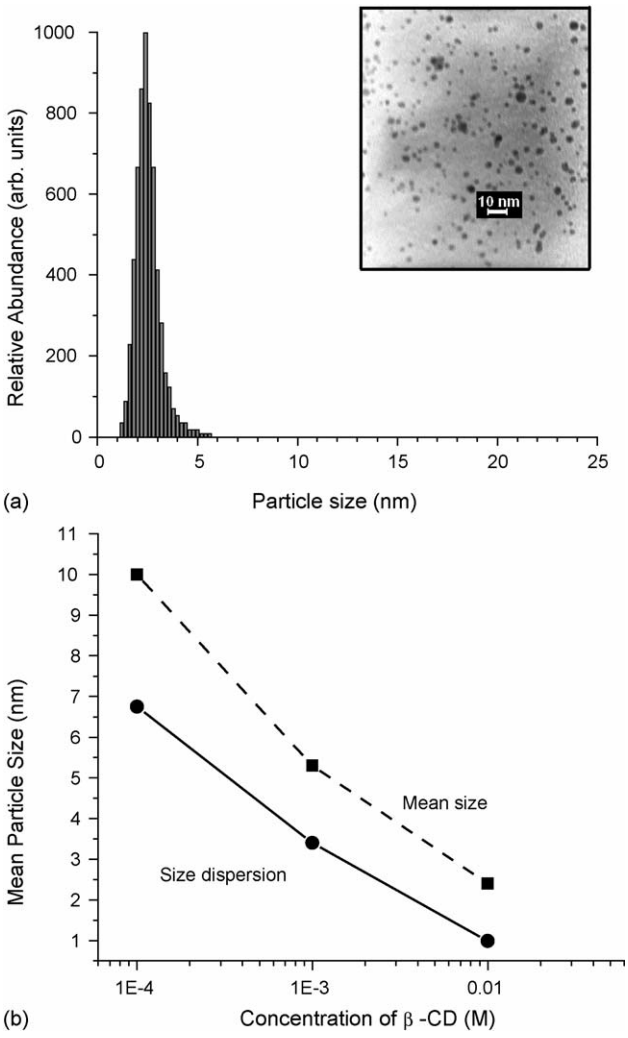

Fig. 2. TEM micrograph images and corresponding size distributions of gold particles prepared by the femtosecond laser ablation in 0.01 M β-CD (a) effect of the β-CD concentration on the resulting average particle size and the size dispersion at FWHM (b).

CDs, consisting of six, seven and eight units, respectively) [25]. Their interior cavity, as well as the primary face, is hydrophobic, while the secondary face and exterior surface are hydrophilic. In our experiments, a drastic size reduction was observed when the concentration of CDs increased, with the smallest size and narrowest dispersion for β-CD, followed by γ-CD and α-CD. Fig. 2 illustrates the effect of the reduction of nanoparticle mean size and size dispersion as the concentration of β-CD increases. As shown in Fig. 2(a), the ablation in highest concentrations of β-CD (10 mM) produced particles with the mean size of 2.1–2.3 nm with dispersion less than 1 nm FWHM. This distribution corresponded to a deep red color of the solution. The colloidal solutions were extremely stable, while no traces of glucose, a major degradable product of CDs was present in the solution after the ablation process, suggesting that CD molecules remained intact during the course of experiment.

Such a striking effect of CDs on the size reduction and stability of solutions was a pleasant surprise, considering the absence of any obvious chemical interactions between CDs and gold

colloids. To understand the mechanism of reduction, we performed some control tests. In particular, we varied pH of aqueous solutions and examined not only the size distribution, but also surface chemistry and charge of nanoparticles produced [20–22]. This enabled to develop a model of chemical interactions during the fabrication process. In this model, we postulated that the reduction of nanoparticle size during laser ablation in aqueous solutions of CDs is first of all the result of the hydrogen bonding of the –OH groups present on the same face of the CDs and the $-O^-$ at the gold surface and the hydrophobic interaction between the primary face of the CD molecule and the unoxidized gold nanoparticle surface. The CD molecules cover gold nanoclusters just after ablation and act like "bumpers", limiting contact between particles, preventing their coalescence (when the particles are still "hot") and aggregation (when the particles are "cold"). It is important that gold nanoparticles prepared with CDs can be biofunctionalized. Indeed, the interior hydrophobic cavity of CDs can still be used for immobilization of different biological species such as some hydrophobic drugs. This gives a promise for potential applications of nanoparticle-CD complexes in biosensing tasks.

Similar effect of the reduction of nanoparticle size down to 3–7 nm was observed when biopolymers (dextrans, PEG) were used as reducing agents [26]. In this case, the size reduction and stabilization of solutions mainly comes from the hydrogen bounding between the partially oxidized gold surface and the OH group of the stabilizing agents. Furthermore, binding interactions of different OH groups of dextrans with Au surface can lead to the reinforcement of the resulting effect.

Thus, OH groups of different biocompatible compounds (polysaccharides, biopolymers) can efficiently react with oxidized gold surface leading to the reduction of the nanoparticle size. Furthermore, the ultra-pure laser-ablated nanoparticles can be functionalized by a proper chemical modification of chemicals. We believe that this gives a huge advantage over the chemically produced nanoparticles for nano-engineering and functionalization of nanoparticles produced, as well as for a solution of toxicity problems.

3.2.3. Amine group

n-Propylamine was specifically selected as a model study to investigate interactions between nanoscale Au colloids and the amine group. Ablation (250 mJ/pulse) in 10 mM *n*-propylamine resulted in bright red gold sols after several minutes, indicating the formation of small gold particles. The sols were also stable for several months when stored in capped bottles, at room temperature. TEM measurements (Fig. 3) confirmed that particles with a mean size of 5–8 nm and a dispersion of less than 4–7 nm were produced. In order to better understand the nature of the interaction, XPS studies were carried out. A high resolution Au4f spectrum was obtained (not shown) and was almost identical to the one obtained for gold in pure water. High resolution N1s spectra were also obtained for samples as-prepared and after being dialyzed for 5 days to eliminate unbonded *n*-propylamine. The experimental spectra were separated into two peaks, one at about 402.3 eV, attributed to ammonium ion ($-NH_3^+$), and another at about 400.6 eV, attributed to amine

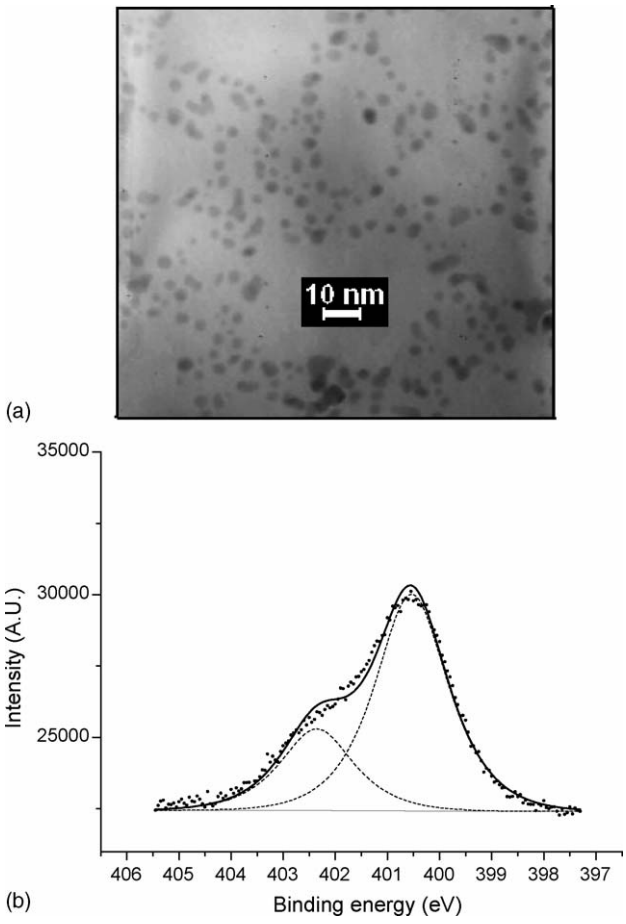

Fig. 3. (a) TEM micrograph image of gold particles prepared by the femtosecond laser ablation of gold in *n*-propylamine; (b) high resolution XPS spectra of the nitrogen (N1s) peak of gold nanoparticles produced by laser ablation in 10 mM aqueous solution of propylamine after 5 day dialysis.

($-NH_2$). Notice that the ammonium ion is dominant in the undialyzed sample, while the amine dominates subsequent to dialysis. This is a strong indication that the unprotonated *n*-propylamine is chemisorbed to the gold particles surface while the ammonium ion interacts electrostatically with the negatively charged nanoparticles. These electrostatic interactions are sufficiently strong for the protonated *n*-propylamine to remain bound to the gold even under the high vacuum conditions of the XPS, but cannot withstand extensive dialysis.

4. Conclusions

We developed femtosecond laser ablation-based methodologies for a production of small and almost monodispersed colloidal gold nanoparticles in aqueous biocompatible solutions. Having partially oxidized surface and free of any contaminants, the laser-ablated nanoparticles exhibit unique surface chemistry. In particular, we showed that they are capable of efficiently interacting with OH and amine groups of different chemicals (e.g., polysaccharides, biopolymers, etc.), whereas interactions with the thiol group are much weaker. Such unique surface chemistry opens novel opportunities for the engineering and functional-

ization of newly synthesized nanomaterials for biosensing and imaging applications.

Acknowledgements

We acknowledge the financial contribution from the Natural Science and Engineering Research Council of Canada and Canadian Institute for Photonics Innovations (CIPI). The authors thank J.-P. Sylvestre, S. Besner, E. Sacher, S. Poulin of Ecole Polytechnique, J.H.T. Luong of Biotechnology Research Institute (Montreal), who were involved in activities of this research project.

References

[1] M. Kerker, The Scattering of Light and other Electromagnetic Radiation, Academic Press, New York, 1969.
[2] U. Kreibig, M. Vollmer, Opt. Properties of Metal Clusters, Springer-Verlag, Berlin, 1996.
[3] M.A. Hyatt (Ed.), Colloidal Gold: Principles, Methods, and Applications, vol. 3, Academic Press, New York, 1989.
[4] A. Fojtik, et al., Bunsenges. Phys. Chem. 88 (1984) 969.
[5] C.T. Dameron, et al., Nature 338 (1989) 596.
[6] D.W. Thompson, I.R. Collins, J. Colloid Interface Sci. 152 (1992) 197.
[7] A.M. Derfus, Nano Lett. 4 (2004) 11.
[8] X. Michalet, et al., Single Mol. 2 (2001) 261.
[9] A. Fojtik, A. Henglein, Ber. Bunsen-Ges. Phys. Chem. 97 (1993) 252.
[10] M.S. Sibbald, G. Chumanov, T.M. Cotton, J. Phys. Chem. 100 (1996) 4672.
[11] M.S. Yeh, Y.S. Yang, Y.P. Lee, H.F. Lee, Y.H. Yeh, S. Yeh, J. Phys. Chem. 103 (1999) 6851.
[12] F. Mafune, J.-Y. Kohno, Y. Takeda, T. Kondow, H. Sawabe, J. Phys. Chem. B 104 (2000) 9111.
[13] F. Mafune, J.-Y. Kohno, Y. Takeda, T. Kondow, H. Sawabe, J. Phys. Chem. 104 (2000) 8333.
[14] F. Mafune, J.-Y. Kohno, Y. Takeda, T. Kondow, H. Sawabe, J. Phys. Chem. B 105 (2001) 5144.
[15] Y.-H. Chen, C.-S. Yeh, Colloids Surf. 197 (2002) 133.
[16] S.I. Dolgaev, A.V. Simakin, V.V. Voronov, G.A. Shafeev, F. Bozon-Verduraz, Appl. Surf. Sci. 186 (2002) 546.
[17] T. Tsuji, K. Iryo, N. Watanabe, M. Tsuji, Appl. Surf. Sci. 202 (2002) 80.
[18] A.V. Kabashin, M. Meunier, C. Kingston, J.H.T. Luong, J. Phys. Chem. B 107 (2003) 4527.
[19] A.V. Kabashin, M. Meunier, J. Appl. Phys. 94 (2003) 7941.
[20] J.-P. Sylvestre, A.V. Kabashin, E. Sacher, M. Meunier, J.H.T. Luong, J. Am. Chem. Soc. (Commun.) 126 (2004) 7176.
[21] J.-P. Sylvestre, A.V. Kabashin, E. Sacher, M. Meunier, J. Luong, Proc. SPIE 5339 (2004) 84.
[22] J.-P. Sylvestre, S. Poulin, A.V. Kabashin, E. Sacher, M. Meunier, J.H.T. Luong, J. Phys. Chem. B 108 (2004) 16864.
[23] J.-P. Sylvestre, A.V. Kabashin, E. Sacher, M. Meunier, Appl. Phys. A 80 (2004).
[24] T. Sakka, S. Iwanaga, Y.H. Ogata, A. Matsunawa, T.J. Takemoto, Chem. Phys. 112 (2000) 8645.
[25] J. Szejtli, in: J.L. Atwood, J.E.D. Davies, D.D. Macnicol, F. Vogtle (Eds.), Comprehensive Supramolecular Chemistry, vol. 3, Pergamon-Elsevier, New York, 1996, pp. 5–40.
[26] S. Besner, A.V. Kabashin, M. Meunier, F.M. Winnik, Proc. SPIE 5969 (2005) 31.